Diaphragmatic Surface Reconstruction from MR Temporal Sequences of Images

Leonardo Ishida Abe, ishida.leonardo@gmail.com
José Miguel Manzanares Chirinos, jmig.kat@gmail.com
Neylor Antunes Stevo, neylorstevo@gmail.com
Renato Seiji Tavares, reseta@uol.com.br
Marcos de Sales Guerra Tsuzuki, mtsuzuki@usp.br
Computational Geometry Laboratory, Escola Politécnica da USP, Brazil

Toshiyuki Gotoh, gotoh@sci.ynu.ac.jp
Seiichiro Kagei, kagei@ynu.ac.jp
Yokohama National University, Japan

Tae Iwasawa
Kannagawa Cardiovascular and Respiratory Centre, Japan

Abstract. The diaphragm is a flat muscle sheet and it is the biggest respiratory muscle. It is alone responsible for most of the volume changes during quiet, and to a somewhat lesser degree, during forced respiration. The quantification of true diaphragmatic motion is challenging, but at the same time a promising field of investigation in MRI of the lung. Compared to CT, MR imaging involves longer acquisition times and it is preferable because it does not involve radiation. On the other hand, MRI is hampered by several challenges: the low amount of tissue relates to a small number of protons leading to low signal, countless air-tissue interfaces cause substantial susceptibility artifacts, and respiratory and cardiac motion cause blurred imaging. MR signal is generated from protons within water molecules and organic material. The lung parenchyma contains only about 800 g of tissue and blood, which is distributed over a volume of 4 to 6 liters. Proton density and signal intensity are therefore extremely low compared to other parts of the body. Several groups used static MRI at different respiratory volumes to gain further insight into the function of the diaphragm. Images were acquired during a breath hold with a relaxed diaphragm in sagittal and coronal orientation. Most of the time during the respiratory cycle, the diaphragm is in motion, either actively contracting during inspiration or passively expanding during expiration. To truly understand its mode of function in contributing to lung volume changes, static analysis as described in the previous section is not ideal. This work proposes a method to reconstruct the 3D diaphragmatic movement from coronal and sagittal temporal sequences of MRI. It is known that the lung movement is not periodic and it is susceptible to variations in the degree of respiration. As coronal and sagittal sequences of images are orthogonal to each other, their intersection corresponds to a segment in the three dimensional space. A time sequence of this intersecting segment can be stacked, defining a two dimension spatio temporal image. The proposed method searches for breathing patterns present in spatio temporal images extracted from the intersection line between a coronal and sagittal sequences of temporal MRI. The breathing patterns are determined by assuming that the diaphragmatic movement is the principal movement and all the lungs structures do move almost synchronously. The synchronization was realized through a pattern named respiratory function. A Hough transform algorithm, using the respiratory function as input, searches for synchronized movements with the respiratory function. The temporal registration determines the instants with the same diaphragmatic level at the intersecting line. The registration is done without the use of any triggering information and any special gas to enhance the contrast. The temporal sequences of images are acquired in free breathing. Several results and conclusions are shown.

Keywords: MR imaging, movement of the lung, interval arithmetics, Hough transform, active contour.

1. INTRODUCTION

The lung presents some characteristics that do not allow its movement direct observation. The use of devices for obtaining images of internal organs is the only way to view the lung movement. Currently, several techniques for modeling the movement of the lung during respiration, exclusively based on CT images, have been proposed (Lujan *et al.*, 1999; van Herk, 2004; Keall *et al.*, 2005; Sarrut *et al.*, 2007). The large FOV (Field of View) of the lung, however, makes repeated use of these systems prohibitive due to high radiation exposure.

Considering the safety of subjects, MR devices are preferable. Moreover, MR is hampered by several aspects: the small amount of tissue refers to a small number of protons leading to signs with poor quality, several interfaces of air layer cause substantial artifacts, and respiratory and cardiac motion cause the blurring. The MR signal is generated from the protons in water molecules and organic material. Lung parenchyma contains only about 800 g of tissue and blood, which is distributed in a volume of 4 to 6 liters. However, the proton density and signal intensity are extremely low compared to
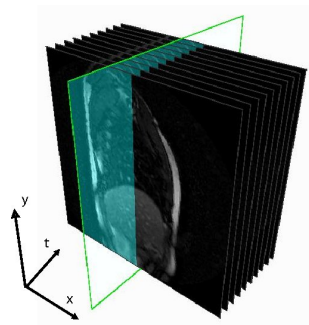
Figure 1. Illustration of an arbitrary intersection parallel to the time axis with an STV.
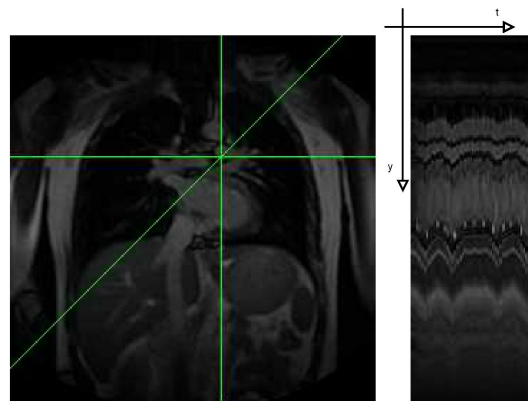

Figure 2. Example of MR image of the chest and a 2D vertical spatio-temporal (2DST) image.

other parts of the body.

The rapid movement of body structures (for example, the pulsating movement of liquid within the vessels) during MR measurements results in inconsistencies in phase and amplitude of the magnetization. This disorder affects magnetization in the imaging of these structures, making them visible only in some instants (blurring and ghosts). Sequences with balanced steady state free precession (SSFP) as the TrueFISP sequence (True Fast Imaging with Steady-state free Precession) are particularly suitable for obtaining MR images of the lung because of its high SNR (Signal to Noise Ratio) efficiency (Kauczor, 2009).

Few papers analyze the motion of the lung using MR images. Iwasawa *et al.* (2002) evaluated quantitatively the movement of the diaphragm by analyzing the total movement of the diaphragm in a respiratory cycle. The movement of the lungs and its variation in time is of particular interest, and approaches to gain this knowledge were proposed. Cluzel *et al.* (2000) managed to obtain a 3D MR image of the lung with breath hold, shortening the exposure time for each image. Gauthier *et al.* (1994) evaluated not only the area of the diaphragm, but also the shape of the diaphragm at different lung volumes and Gierada *et al.* (1995) considered the diaphragmatic motion using MR sequential images taken during a quiet breathing. Nakamura *et al.* (2005) and Tsuzuki *et al.* (2009) investigated the temporal registry of vectorial coronal and sagittal lung silhouettes extracted from MR images. A vectorial lung silhouette is extracted through different approaches, resulting in polygonal representations for coronal and sagittal silhouettes. An animated 3D model of the lungs is created by composing the silhouettes representing coronal and sagittal planar cross sections. Haneishi *et al.* (2009) created an animated 3D model by correlating sagittal slices and a specially chosen coronal slice through a pattern matching algorithm. Oechsner *et al.* (2009) proposed a technique for the acquisition of temporal sequences of images free of artifacts using navigator echos that are focused at the apex of the hemidiaphragm, and the position of the diaphragm is monitored to determine the level of inflation. Singh *et al.* (2008) used dynamic sequences of MR images to create a 4D representation of the swallowing process in which, sagittal and coronal slices were recorded versus time.
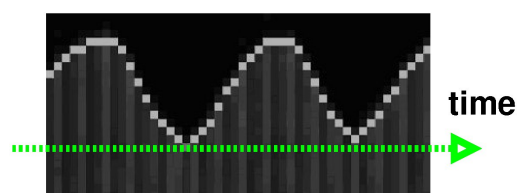

Figure 3. A standard $f_s(t)$ respiratory function.

There are essentially two different approaches to register images of respiratory movement. The static approach uses standard image sequences, which are obtained with breath holding at different instants, and this is repeated to obtain images in at least two different respiratory positions. It has the advantage of providing anatomical details that are useful for further analysis, as the application of registration algorithms. The disadvantage is that the lung may reach a state of tension and pressure with uniform distribution when the breath is held (Kauczor, 2009). The second approach, which is used in this work, uses rapid imaging to capture images during free breathing. Unfortunately, the gains in speed always leads to a reduction in detail.

In this paper, the animated diaphragmatic surface is reconstructed using several coronal and sagittal MR sequences of images. Section 2 explains how synchronous movement patterns are automatically determined by the Hough transform algorithm. An active contour algorithm is used to adjust small discrepancies created by the synchronicity restriction. The diaphragmatic respiratory patterns are manually determined. In the following, the temporal registration algorithm, based on diaphragmatic surface level and respiratory phase is explained. As time is a discrete variable, it is not possible to ensure that the temporal registration can be realized in all situations. The used approach can determine if the temporal registration can be done using the given sequence of images. If it is not the case, the algorithm determines between which two images the registration should happen and how far the registration is. The registration algorithm is explained in section 3. Section 4 shows some results and section 5 presents the conclusions.

2. Respiratory Patterns

In the case of the lung, a volumetric 3D description can not be obtained by MR. As the MR imaging process is slow, it is possible to obtain temporal sequences of images representing 2D slices in 3D space. The image on each slice is obtained at different time instants, with the lungs in different states of inhalation and exhalation. In this section, the temporal registration based on respiratory patterns is explained.

2.1 Standard Respiratory Function

A temporal sequence of MR images of the lung can be stacked, defining a spatio-time volume (STV) $I(x, y, t)$, where x and y are pixel coordinates and t is time. Consider an arbitrary plane α, parallel to t and y axis, which passes through a point (x_s, y_s). The intersection of STV $I(x, y, t)$ with the arbitrary plane α defines a 2D spatio-temporal (2DST) image as illustrated in Fig. 1. Fig. 2 displays a vertical 2DST image. One can see the presence of movement patterns associated with internal structures and organs boundaries.

A standard $f_s(t)$ respiratory function is determined around the diaphragmatic region. The diaphragmatic surface is easier to observe with a good contrast, since its motion has a larger amplitude when compared to other thoracic structures. A $f_s(t)$ is shown in Fig. 3, representing a sequence of nonnegative integer values in time. A $f_s(t)$ is within the range $[0, f_{max}]$, where f_{max} is the maximum amplitude.

Therefore, the standard respiratory function is an estimate of pulmonary structures movement in an 2DST image. It is the input to the Hough transform to determine the presence of synchronous movements during free breathing. The Hough transform is applied to edge images.

2.2 Hough Transform as a Tool to Find Respiratory Patterns

The Hough transform is a feature extraction technique used in image analysis, computer vision and digital imaging (Duda and Hart, 1972; Kiryati *et al.*, 1991). It is usually used to detect straight lines and curves. The aim of the technique is to find instances of imperfect patterns through a voting procedure. A new Hough transform was proposed by Matsushita *et al.* (2004) to determine the presence of respiratory patterns $f_k(t)$ in 2DST images. It is assumed that each point moves in time according to a standard respiratory function up to a scale and an offset. Hence, the temporal movement is described by

$$f_k(t) = y = a \cdot f_s(t) - b \tag{1}$$

where a and b are scale and offset of $f_s(t)$, respectively. The search for respiratory patterns $f_k(t)$ can be summarized as the identification of a large set of pairs (a, b) for the largest possible number of 2DST images for a given STV. The Hough transform uses edge images to determine the presence of respiratory patterns associated with internal structures and organs boundaries.

An edge image is determined from a 2DST image using a gradient filter (Heath *et al.*, 1998). A respiratory pattern is fully specified by a pair (a, b). To detect a respiratory pattern, the Hough transform maps each edge pixel (t, y) from the 2DST image into lines in the quantized space (a, b), where contributions from each pixel (t, y) to the quantized space (a, b) are accumulated. A matrix is used to represent the quantized space. Each pixel (t, y) in 2DST edge image represents a line in quantized space, the cells where the line passes are adequately incremented. This process is repeated for all edge pixels. Every cell within the quantized space maps a respiratory pattern in the 2DST image.
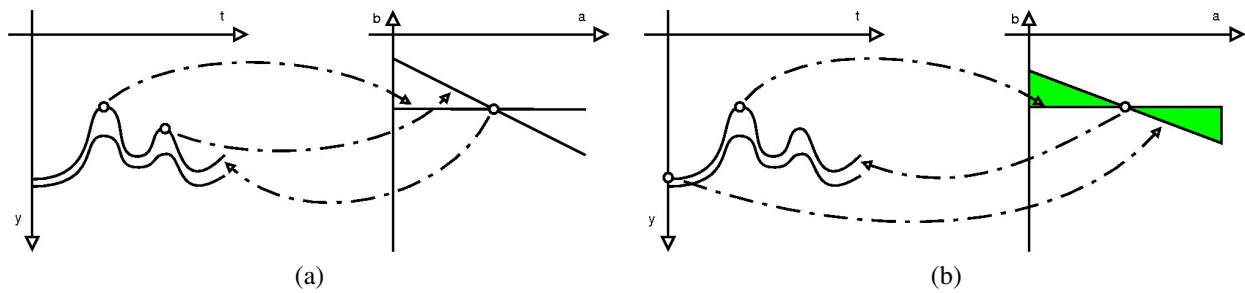
Figure 4. (a) The Hough transform, the 2DST image is on the left and the quantized space is on the right. The respiratory pattern in the 2DST image is mapped to a cell in the quantized space. (b) The region that needs to be re-sampled is displayed in green. This region contains all lines that pass through the cell with greater intensity and has slope internally to the range $[0, f_{max}]$.

Thus, the intensity of each cell (a, b) in the quantized space is associated with the probability of finding a respiratory pattern. Fig. 4.(a) displays two pixels from a 2DST image that were mapped to two lines in the quantized space. These two lines intersect at a cell in the quantized space, this cell is mapped to a respiratory pattern containing both original pixels in the 2DST image. The cell with higher value has greater confidence representing a respiratory pattern. Assuming that this cell is (a_1, b_1), the following respiratory pattern is represented

$$y = f_k(t) = a_1 \cdot f_s(t) - b_1. \tag{2}$$

To make the search for others respiratory patterns, it is assumed that no internal organs intersect each other. Consequently, no intersection of respiratory patterns is allowed. The pixels belonging to the just found respiratory pattern are re-sampled with negative values and the quantized space is updated. In this process, all respiratory patterns that intersect the just found respiratory pattern, are removed. This process can be defined by noting that $f_s(t)$ is limited by the interval $[0, f_{max}]$, which defines the limits of the straight line slope in the quantized space, as shown in expression (2). Thus, any line passing through (a_1, b_1) in the quantized space with angular coefficient internal to the interval $[0, f_{max}]$ must be re-sampled negatively, or have their pixel intensity set to zero in the quantized space (see Fig. 4.(b)). As all intersecting respiratory patterns were removed, a new peak in the quantized space can be found and the re-sampling process can be performed again. This process is repeated as many times as necessary.

Usually, image processing algorithms assume that a pixel represents an exact location. In practice, discreteness prevails; in the input stage, the data is obtained from a discrete domain (for example, by MR scanners). In the quantization stage, the algorithm is computed using an accumulating matrix that is discrete. However, it is theoretically supposed to be continuous. In this scenario, the algorithm that does not take into account such discreteness, often fails with severe consequences. Tavares *et al.* (2009) improved the Hough transform by applying interval arithmetics.

2.3 Active Contour Algorithm (Snakes)

The Hough transform determines synchronized movements in the 2DST image, however it is known that the lung movement is not totally synchronous. The active contours algorithm proposed by Kass *et al.* (1987) removes the synchronicity restriction. In this algorithm a curve is defined within the image domain and it moves under the influence of internal and external forces. These forces are defined so that the curve deforms and converges to the contour of a desired object in the image.

In this work, it is used the greedy snake algorithm proposed by Williams and Shah (1992). The greedy snake algorithm is more stable and shows a considerable improvement in the speed of convergence of the curve compared with the original method. The respiratory pattern resulting from the Hough transform is the initial guess for the active contours algorithm. A respiratory pattern $f_k(t)$ is a set of pixels with only one pixel for each vertical line (see Fig. 5) and it is given by

$$f_k(t) = \{y_1, y_2, \cdots, y_n\}$$

where $1 \leq t \leq n$, n is the number of frames. The energy function to be minimized is defined as

$$E(f_k(t)) = E_{int}(f_k(t)) + E_{image}(f_k(t))$$

where E_{int} is the internal energy and it is defined as

$$E_{int}(f_k(t)) = \frac{1}{2} \left(\alpha \cdot |\frac{\partial f_k(t)}{\partial t}|^2 + \beta \cdot |\frac{\partial^2 f_k(t)}{\partial t^2}|^2 \right) \tag{3}$$
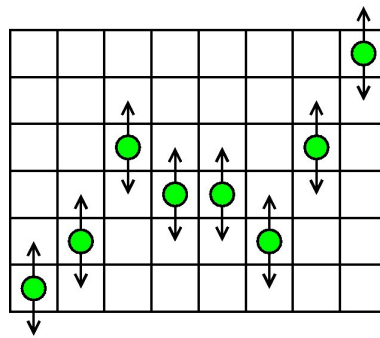
Figure 5. A respiratory pattern resulting from the Hough transform. The active contours algorithm searches for a position of smaller energy in the vertical adjacency of the pixels belonging to the respiratory pattern.

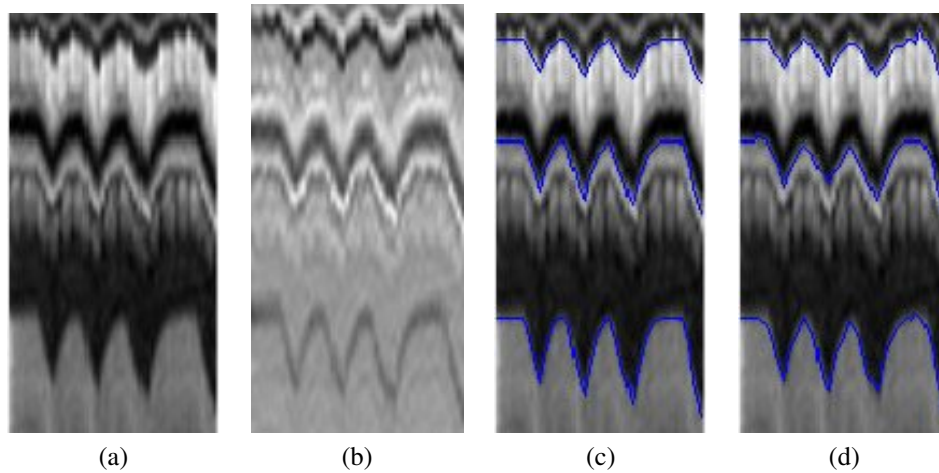(a)   (b)   (c)   (d)

Figure 6. (a) The original 2DST image. (b) The edge image. (c) Respiratory pattern detected by the Hough transform. (d) Respiratory pattern detected by the active contours algorithm.

where α and β are positive parameters. E_{image} is the term that attracts the respiratory pattern to the pixels with higher intensity in the edge image. It is defined as

$$E_{image}(f_k(t)) = -\frac{\gamma}{\sigma(f_k(t))} \cdot |\nabla I(f_k(t))| \qquad (4)$$

where γ is a positive parameter, $\sigma(F_k(t))$ is the pixel intensity standard deviation of the pixels that define the respiratory pattern candidate and $\nabla I(F_k(t))$ is the edge pixel intensity average of the edge pixels that define the respiratory pattern candidate. The algorithm initially analyzes the odd verticals and in the sequence the even verticals. In the search of respiratory patterns with smaller energy, the vertical adjacency of each pixel present in the respiratory pattern is analyzed. The process is repeated until no change occurs. Fig. 6 shows the result of the active contours algorithm. It was empirically observed that the contribution of the image component $E_{image}(f_k(t))$ has a greater influence on the final result. We decided to maintain the ratio $\gamma/\alpha = \gamma/\beta > 1.0$ constant. The values used in this study were $\alpha = 0.7$, $\beta = 0.7$ and $\gamma = 1.2$. The Hough transform and the active contours algorithm were used to determine the lung contour in temporal sequences of coronal and sagittal images by Tavares *et al.* (2010).

2.4 Temporal Registration

Stevo *et al.* (2009) proposed a coronal sagittal mapping where the segment associated with the intersection between sagittal and coronal images. Fig. 7 shows two sequences of images: coronal and sagittal. Fig. 7.(a) (Fig. 7.(c)) shows a vertical line representing the intersection of this coronal (sagittal) sequence with the sagittal (coronal) sequence of images. Both verticals represent the same segment in the 3D space. The 2DST image extracted from the coronal (sagittal) sequence of images at this position is shown in Fig. 7.(b) (Fig. 7.(d)). A temporal registration happens when a fixed coronal (sagittal) image and a sagittal (coronal) temporal sequence of images are given. The registration algorithm searches for a frame from the sagittal (coronal) temporal sequence of images that fits the given fixed sagittal (coronal) image. Fig. 7.(e) shows a temporal registration where the frame from the coronal sequence that fitted the fixed sagittal image was determined.

Stevo *et al.* (2009) proposed two fitting algorithms based on discrete Fourier transform and pixel by pixel comparison.
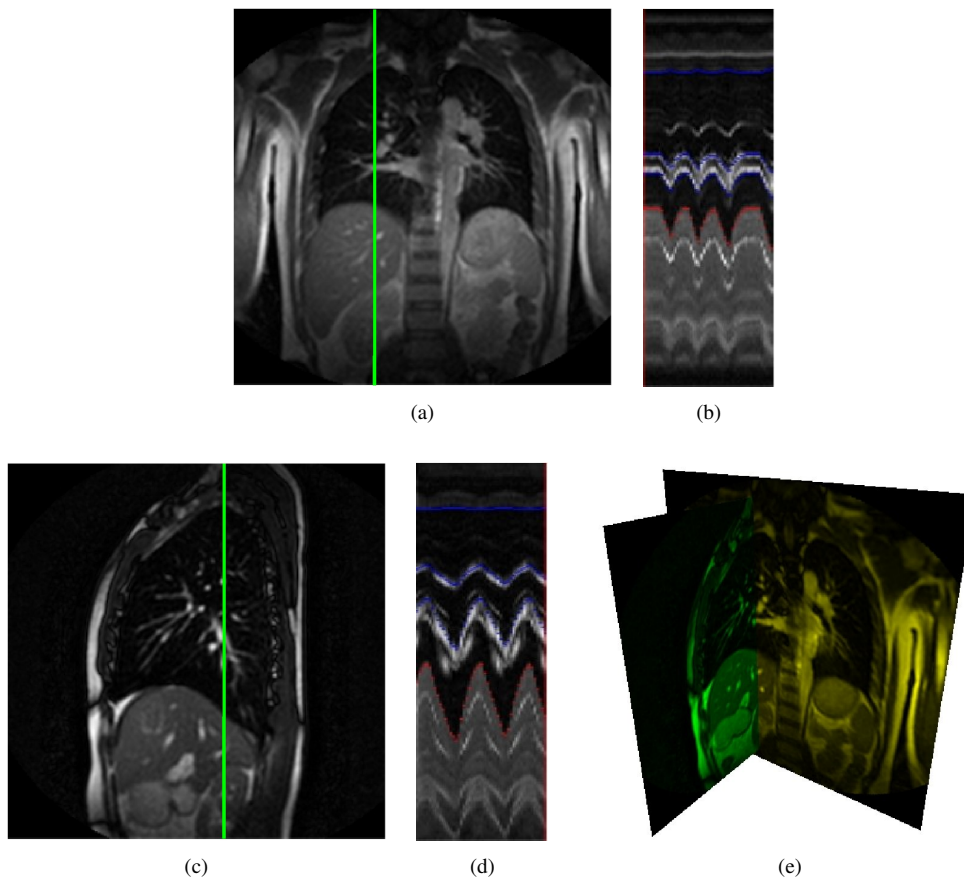
Figure 7. (a)-(b) The coronal image has a vertical line showing where the 2DST image was obtained. 21 respiratory patterns were found by the Hough Transform algorithm. (c)-(d) The sagittal image has a vertical line that shows where the 2DST image was obtained. 21 respiratory patterns were found by the Hough Transform algorithm. (e) Result of the temporal registration algorithm.
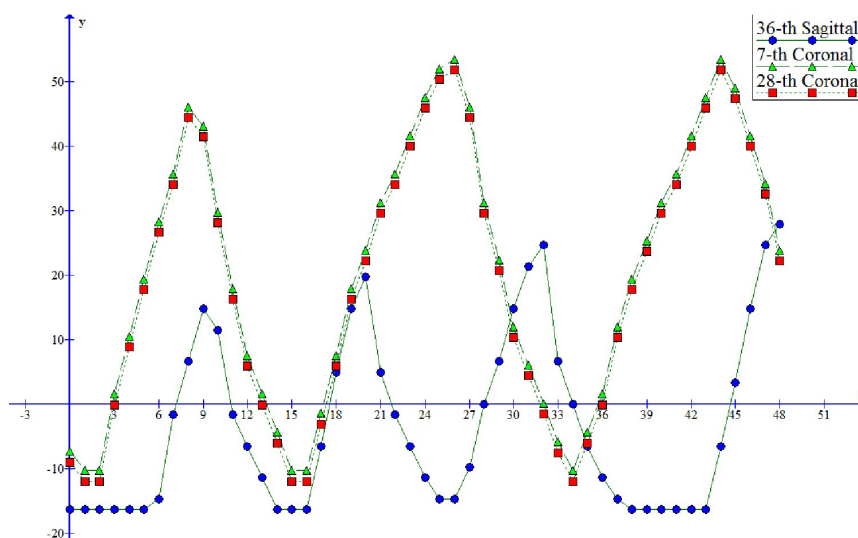

Figure 8. Each graph compares the diaphragmatic level of a fixed sagittal (coronal) image and the diaphragmatic respiratory pattern extracted from a coronal (sagittal) temporal sequence of images. The fixed images used in this graph are 37-th sagittal image, 7-th and 28-th coronal images. Graph 36–sagittal is a coronal diaphragmatic respiratory pattern subtracted from the diaphragmatic level from the 36–th sagittal image. The other graphs are similarly constructed.

(a)   (b)
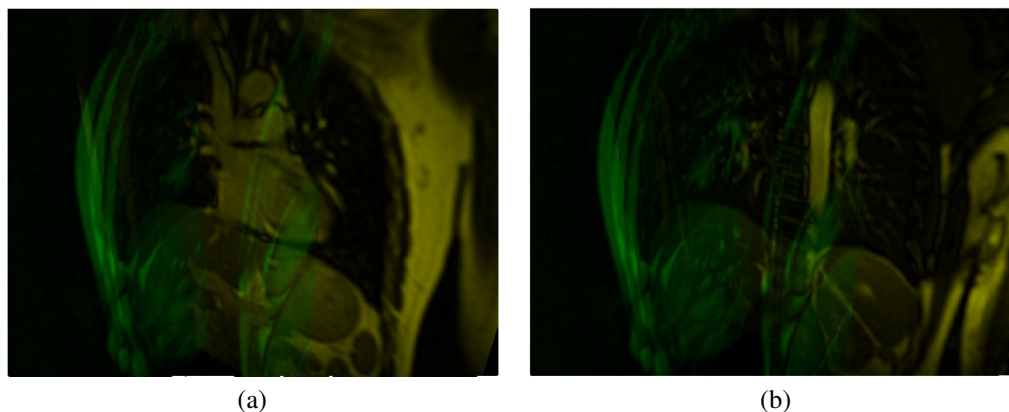
Figure 9. (a) Four sagittal images were registered with a coronal image. All images are in the same breathing phase with the same diaphragmatic level. (b) The same four sagittal images shown in (a) were registered to another coronal image in the same breathing phase.

This algorithm is solely based on the intensity of the pixels which are strongly affected by the blurring and ghosting. Sato *et al.* (2011) proposed a fitting algorithm where the diaphragmatic surface level and the respiratory phase from the fixed image are compared to the diaphragmatic respiratory pattern and respiratory phase (inspiration or expiration) from the temporal sequence. A temporal registration happens when diaphragmatic level and respiratory phase from the fixed image and a frame from the temporal sequence of images match.

Fig. 8 shows diaphragmatic respiratory patterns subtracted from a diaphragmatic level. The diaphragmatic level is obtained from the fixed image and represents the level of the diaphragmatic surface at the intersecting segment with the temporal sequence of images. The diaphragmatic respiratory patterns are extracted from Fig. 7.(b) and (d). Fig. 8 shows two diaphragmatic respiratory patterns subtracted from three diaphragmatic levels. When a curve crosses the x axis means that a temporal registration happens. One can observe that 28–th coronal and 36–th sagittal are a temporal registration pair. Stevo *et al.* (2010) used this algorithm to determine several coronal (sagittal) images that fits a given sagittal (coronal) image. Fig. 9 shows an example of the multiple registration algorithm.

As time is a discrete variable, it is possible that there is no image to realized the temporal registration. The approach proposed by Sato *et al.* (2011) can determine if such situation happens and between which two frames the temporal registration must happen. This situation is illustrated by graph 7–th coronal in Fig. 8. The registration for the fixed 7–th sagittal must happen between the 35–th and 36–th frames from the sagittal sequence.

3. Diaphragmatic Surface Reconstruction

The diaphragmatic surface can be reconstructed by applying the temporal registration algorithm several times. The situation where the diaphragmatic respiratory pattern cannot be fitted is solved by determining the fitting position as an interpolation and the diaphragmatic silhouette is translated to the interpolated position. Fig. 10 shows the proposed algorithm. Considering that a sagittal sequence of MR images is fixed. There are 12 sagittal and 9 coronal MR temporal sequences of images. The registration happens by comparing 2DST images from the 9 coronal MR temporal sequences with the diaphragmatic level of the fixed sagittal image.

4. Results

The MR image sequences used in the experiment were obtained by Symphony (1.5T) made by Siemens, using True-FISP. MR images were obtained from six healthy nonsmokers. Table 1 shows some characteristics of the subjects and sequences. Initial images in dynamic data sets were acquired in the transient state of magnetization, so they have high signal intensity and different contrast. The analysis included all acquired images, including the initial images. Fig. 7 shows an example of the Hough transform result where several respiratory patterns were found. In this work, it was used 25 sagittal and 31 coronal sequences of images from the same subject obtained at different instants of time, and each image sequence has 50 images. Figs. 11.(a)-(d) show the diaphragmatic surface reconstructed based on four distinct fixed sagittal images.

Several authors make strong assumptions on the regularity of respiratory movement and parameterize the respiratory motion as one respiratory period, very similar to standard lung function proposed here. They merge all images that are in the same respiratory phase and consider all collected images belonging to a single respiratory period. Though breathing clearly shows a repetitive nature, reducing the strain of respiratory organs to just one respiratory period ignores the complex variability of the organs and in some cases it may be a very rough approximation. This leads to artifacts
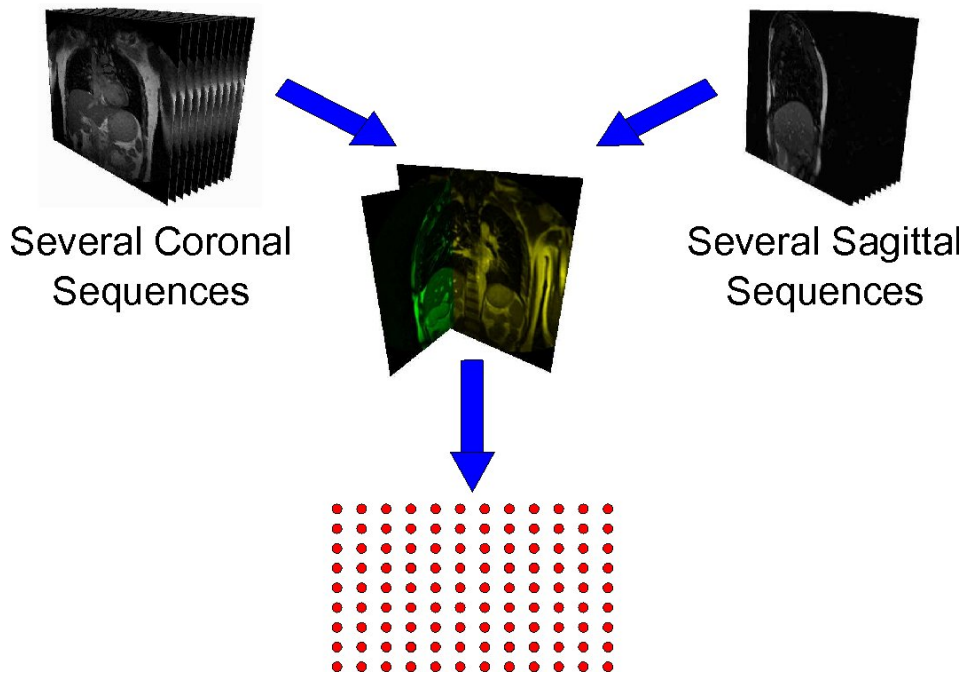
Figure 10. The diaphragmatic surface is reconstructed by applying the temporal registration algorithm at every intersecting segment. In this example, there are 12 sagittal and 9 coronal temporal sequences of images. Initially, the fixed sagittal (coronal) image is selected. Its associated diaphragmatic levels and respiratory phase at the intersecting segments with all coronal (sagittal) temporal sequences are determined. The corresponding diaphragmatic level and respiratory phase is compared with the coronal (sagittal) diaphragmatic respiratory pattern and a registration frame is determined.
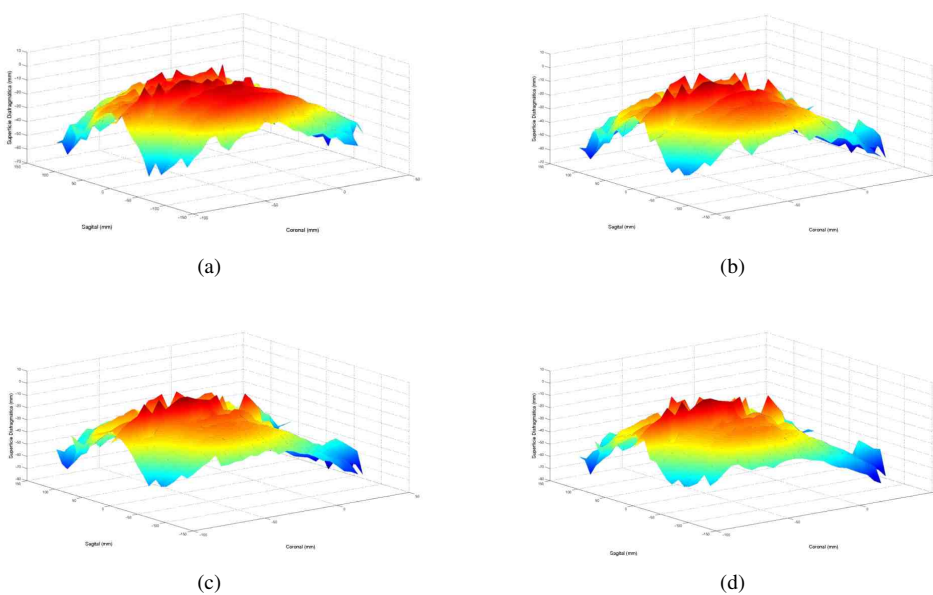

Figure 11. (a)-(d) Sequence of four reconstructed diaphragmatic surfaces based on fixed sagittal images.

Table 1. Characterization of the MR coronal and sagittal image sequences used in the experiments obtained from six healthy subjects. All sequences have 256×256 pixels, repetition time of $2.33\ ms$, echo time of $1.16\ ms$, thickness of $10\ mm$ and the number of images in each sequence is 50

Sub.	fov - cor (mm)	fov - sag (mm)	total time (s)	age
A	420×420	380×380	17	31
B	420×420	380×380	11	31
C	420×420	380×380	11	24
D	450×450	450×450	27	58
E	420×420	380×380	11	50
F	450×450	450×450	11	28

in the reconstructed images and considerable uncertainty (Vedam *et al.*, 2003; Fitzpatrick *et al.*, 2006). In the method proposed in this work, the MR sequence of images are obtained from free breathing and the complete sequence of images is considered by analyzing the diaphragmatic respiratory pattern. Intermediary information is interpolated from two consecutive frames.

von Siebenthal (2008) tracked vascular structures present in liver sagittal images during a complete breathing cycle, and used a "navigator" slice containing transverse vessels that are distributed throughout a slice of the liver and are also easily traceable. He followed the movement of the vascular structures of the liver in 2D space. Several authors have used a similar approach to track the internal structures of the lung in the sequences of images obtained from CT (Sarrut *et al.*, 2007; Coselmon *et al.*, 2004; Rietzel and Chen, 2006; Castillo *et al.*, 2009). In the method proposed in this work, the intersecting segment between coronal and sagittal images is analyzed. This way, variations in time of the diaphragmatic surface movement can be determined and considered in the registration.

The approach proposed here is convinced that the diaphragm was properly constituted in the process of free breathing. When available in both images (coronal and sagittal), the internal structures of the lung are also properly registered. A disadvantage is that, currently, breathing patterns resulting from the Hough transform had to be manually filtered.

5. Conclusions

A method for 3D animated reconstruction of the diaphragmatic surface using MR sagittal and coronal images acquired during free breathing is proposed in this work. The Hough transform in combination with the active contours algorithm determined several respiratory patterns. Respiratory patterns associated with the diaphragmatic surface were determined. The temporal registration based on respiratory patterns associated with the diaphragmatic surface showed to be effective.

6. ACKNOWLEDGEMENTS

7. REFERENCES

Castillo, R, Castillo, E, Guerra, R, Johnson, VE, McPhail, T, Garg, AK and Guerrero, T, 2009. "A framework for evaluation of deformable image registration spatial accuracy using large landmark point sets". *Phys Med Biol*, Vol. 54, pp. 1849–1870.

Cluzel, P., Similowski, T., Chartrand-Lefebvre, C., Zelter, M., Derenne, J.P. and Grenier, P.A., 2000. "Diaphragm and chest wall: assessment of the inspiratory pump with MR imaging–preliminary observations". *Radiology*, Vol. 215, pp. 574–583.

Coselmon, M.M., Balter, J.M., McShan, D.L. and Kessler, M.L., 2004. "Mutual information based CT registration of the lung at exhale and inhale breathing states using thin-plate splines". *Med Phys*, Vol. 31, pp. 2942–2948.

Duda, R.O. and Hart, P.E., 1972. "Use of the Hough transformation to detect lines and curves in pictures". *CACM*, Vol. 15, pp. 11–15.

Fitzpatrick, MJ, Starkschall, G, Antolak, JA, Fu, J, Shukla, H, Keall, PJ, Klahr, P and Mohan, R, 2006. "Displacement-based binning of time-dependent computed tomography image data sets". *Med Phys*, Vol. 33, pp. 235–246.

Gauthier, A.P., Verbatick, S., Estenn, M., Segebartg, C., Macklem, P.T. and Paiva, M., 1994. "Three dimensional reconstruction of the in vivo human diaphragm shape at different lung volumes". *J Appl Physiol*, Vol. 76, pp. 495–50.

Gierada, D.S., Curtin, J.J., Erickson, S.J., Prost, R.W., Strandt, J.A. and Goodman, L.R., 1995. "Diaphragmatic motion: fast gradient–recalled–echo MR imaging in healthy subjects". *Radiology*, Vol. 194, pp. 879–884.

Haneishi, H., Masuda, Y. and Ue, H., 2009. "Dynamic 3D image analysis of thoracoabdominal region". *IEICE Tech Rep*, Vol. 125, pp. 293–297.

Heath, M., Sarkar, S., Sanocki, T. and Bowyer, K., 1998. "Comparison of edge detectors: a methodology and initial study". *Comp Vis Image Und*, Vol. 69, pp. 38–54.

Iwasawa, T., Kagei, S., Gotoh, T., Yoshiike, Y., Matsushita, K., Kurihara, H., Saito, K. and Matsubara, S., 2002. "Magnetic resonance analysis of abonormal diaphragmatic motion in patients with emphysema". *Eur Respir J*, Vol. 19, pp. 225–331.

Kass, M., Witkin, A. and Terzopoulos, D., 1987. "Snakes: active contour models". *Int J Comput Vision*, Vol. 1, pp. 321–331.

Kauczor, H.U., 2009. *MRI of the lung*. Springer–Verlag, Berlim.

Keall, P.J., Joshi, S., Vedam, S.S., Siebers, J.V., Kini, V.R. and Mohan, R., 2005. "Four-dimensional radiotherapy planning for DMLC-based respiratory motion tracking". *Med Phys*, Vol. 32, pp. 942–951.

Kiryati, N., Eldar, Y. and Bruckstein, A.M., 1991. "A probabilistic Hough transform". *Pattern Recogn*, Vol. 24, pp. 303–316.

Lujan, A.E., Larsen, E.W., Balter, J.M. and Haken, R.K.T., 1999. "A method for incorporating organ motion due to breathing into 3D dose calculations". *Med Phys*, Vol. 26, pp. 715–720.

Matsushita, K., Asakura, A., Kagei, S., Gotoh, T., Iwasawa, T. and Inoue, T., 2004. "Shape tracking on chest MR sequence images using respiratory patterns". *J IIEEJ*, Vol. 33, pp. 1115–1122.

Nakamura, C., Asakura, A., Tsuzuki, M.S.G., Gotoh, T., Kagei, S. and Iwasawa, T., 2005. "Three dimensional lung modeling from sequential MR images based on respiratory motion analysis". *IEICE Tech Rep*, Vol. 105, pp. 33–38.

Oechsner, M., Pracht, E.D., Staeb, D., Arnold, J.F.T., Köstler, H., Hahn, D., Beer, M. and Jakob, P.M., 2009. "Lung imaging under free-breathing conditions". *Magn Reson Med*, Vol. 61, pp. 723–727.

Rietzel, E. and Chen, G.T.Y., 2006. "Deformable registration of 4D computed tomography data". *Med Phys*, Vol. 21, pp. 4423–4430.

Sarrut, D., Delhay, B., Villard, P.F., Boldea, V., Beuve, M. and Clarysse, P., 2007. "A comparison framework for breathing motion estimation methods from 4D imaging". *IEEE T Med Imaging*, Vol. 26, pp. 1636–1648.

Sato, A.K., Stevo, N., Tavares, R.S., Tsuzuki, M.S.G., Kadota, E., Gotoh, T., Kagei, S., Asakura, A. and Iwasawa, T., 2011. "Registration of temporal sequences of coronal and sagittal MR images through respiratory patterns". *Biomed Signal Proces Control*, Vol. 6, pp. 34–47.

Singh, M., Cheng, I. and Mandal, M., 2008. "4D alignment of bidirectional dynamic MRI sequences". In *30th Annu Int IEEE EMBS Conf*. Vancouver, Canada, pp. 5893–5896.

Stevo, N., Sato, A.K., Tsuzuki, M.S.G., Gotoh, T., Kagei, S., Asakura, A. and Iwasawa, T., 2010. "Multiple registration of coronal and sagittal MR temporal image sequences based on Hough transform". In *Proc 32nd Annu Int IEEE EBMS Conf*. Buenos Aires, Argentina.

Stevo, N., Campos, R., Tavares, R.S., Tsuzuki, M.S.G., Gotoh, T., Kagei, S. and Iwasawa, T., 2009. "Registration of temporal sequences of coronal and sagittal images obtained from magnetic resonance". In *Proc COBEM 2009 - 20th Int Cong Mech Eng*.

Tavares, R.S., Sato, A.K., Tsuzuki, M.S.G., Gotoh, T., Kagei, S., Asakura, A. and Iwasawa, T., 2010. "Temporal segmentation of lung region MR images sequences using Hough transform". In *Proc 32nd Annu Int IEEE EMBS Conf*. Buenos Aires, Argentina.

Tavares, R.S., Tsuzuki, M.S.G., Gotoh, T., Kagei, S. and Iwasawa, T., 2009. "Lung movement determination in temporal sequences of mr images using hough transform and interval arithmetics". In *Proceedings of the 7th IFAC Symposium on Modelling and Control in Biomedical Systems*. pp. 192–197.

Tsuzuki, M.S.G., Takase, F.K., Gotoh, T., Kagei, S., Asakura, A., Iwasawa, T. and Inoue, T., 2009. "Animated solid model of the lung constructed from unsynchronized MR sequential images". *Computer Aided Design*, Vol. 41, pp. 573–585.

van Herk, M., 2004. "Errors and margins in radiotherapy". *Semin Radiat Oncol*, Vol. 14, pp. 52–64.

Vedam, S.S., Keall, P.J., Kini, V.R., Mostafavi, H., Shukla, H.P. and Mohan, R., 2003. "Acquiring a four-dimensional computed tomography dataset using an external respiratory signal". *Phys Med Biol*, Vol. 48, pp. 45–62.

von Siebenthal, M., 2008. *Analysis and modelling of respiratory liver motion using 4DMRI*. Ph.D. thesis, Eidgenössische Technische Hochschule ETH Zürich.

Williams, D.J. and Shah, M., 1992. "A fast algorithm for active contours and curvature estimation". *Computat Visual Graphical Image Proces*, Vol. 1, pp. 14–26.

8. Responsibility notice

The author(s) is (are) the only responsible for the printed material included in this paper.